PCCP

CORRECTION

View Article Online
View Journal | View Issue

Check for updates

Cite this: *Phys. Chem. Chem. Phys.*, 2019, **21**, 11488

Correction: Influence of permittivity and energetic disorder on the spatial charge carrier distribution and recombination in organic bulk-heterojunctions

Tim Albes * and Alessio Gagliardi*

DOI: 10.1039/c9cp90135c

rsc.li/pccp

Correction for 'Influence of permittivity and energetic disorder on the spatial charge carrier distribution and recombination in organic bulk-heterojunctions' by Tim Albes *et al.*, *Phys. Chem. Chem. Phys.*, 2017, **19**, 20974–20983.

1 Summary

The authors regret a mistake in their previously published paper and would like to communicate a correction.

Throughout the manuscript, the values for the energetic disorder σ that have been investigated were stated to be 0 meV, 30 meV, 50 meV, and 70 meV. Due to a mistake in the implementation, these values need to be rescaled by a factor of $\sqrt{2}$ and therefore correspond to 0 meV, 42.4 meV, 70.7 meV, and 99.0 meV, respectively. For readability, we will refer to them as 0 meV, 40 meV, 70 meV, and 100 meV in the following.

The results in the original manuscript are correct as presented but the values for the disorder need to be re-labeled throughout the text and in the figures. This correction does not change the overall implications and conclusions, namely the interface charge accumulation and the increased recombination at low permittivity ε_r in combination with a large energetic disorder.

2 Detailed correction

In Fig. 1, the charge carrier distribution (CCD) is shown for σ ranging from 40 meV to 100 meV; it replaces Fig. 2 of the original manuscript. The figure is identical except for the labelling of σ. The statement of the figure remains, *i.e.*, large values of σ can make the CCD fluctuate by several orders of magnitude locally.

The quantitative evaluation of interface densities *vs.* bulk densities is shown in Fig. 2 with the corrected axis description for σ; it replaces Fig. 3 of the original manuscript.

Fig. 4 of the original manuscript remains unchanged, but shows the absolute CCDs for σ = 100 meV instead of 70 meV.

Fig. 5 of the original manuscript shows the total recombination R_{tot} and corresponding relative amount of geminate recombination $\frac{R_{\text{gem}}}{R_{\text{tot}}}$ for σ = 100 meV instead of σ = 70 meV. We have added the results for what should have been Fig. 5 in the original manuscript, *i.e.* R_{tot} and $\frac{R_{\text{gem}}}{R_{\text{tot}}}$ at 70 meV, in Fig. 3 for an extended parameter set of the recombination rate a_{ehr} ranging between $10^4\ \text{s}^{-1}$ and $10^9\ \text{s}^{-1}$. It can be seen from Fig. 3a that, while R_{tot} is considerably smaller than at σ = 100 meV, it shows the same trend of being strongly dependent on both ε_r and a_{ehr}. In particular, also here the change in R_{tot} between slight changes of ε_r outweighs orders of magnitude of a_{ehr} and highlights the strong influence of the permittivity on the total recombination. At a disorder of 100 meV, values less than $a_{\text{ehr}} \approx 5 \times 10^4\ \text{s}^{-1}$ were identified at ε_r = 3.5 in order to obtain a sufficiently functioning device with $R_{\text{tot}} < 25\%$. At 70 meV, values up to $a_{\text{ehr}} \approx 10^7\ \text{s}^{-1}$ (corresponding to 100 ns of pair recombination time) lead to $R_{\text{tot}} < 25\%$, which represent a more realistic scenario according to what is found by transient absorption spectroscopy (TAS) measurements.[1] Even for recombination times of 1 ns ($a_{\text{ehr}} = 10^9\ \text{s}^{-1}$), the device is still reasonably functioning with 37.47% of all charges recombining. From Fig. 3b it is evident that also at σ = 70 meV geminate recombination clearly dominates over nongeminate recombination and cannot be neglected as a major loss mechanism.

Department of Electrical and Computer Engineering, Technical University of Munich, Karlstr. 45, 80333 Munich, Germany. E-mail: tim.albes@tum.de

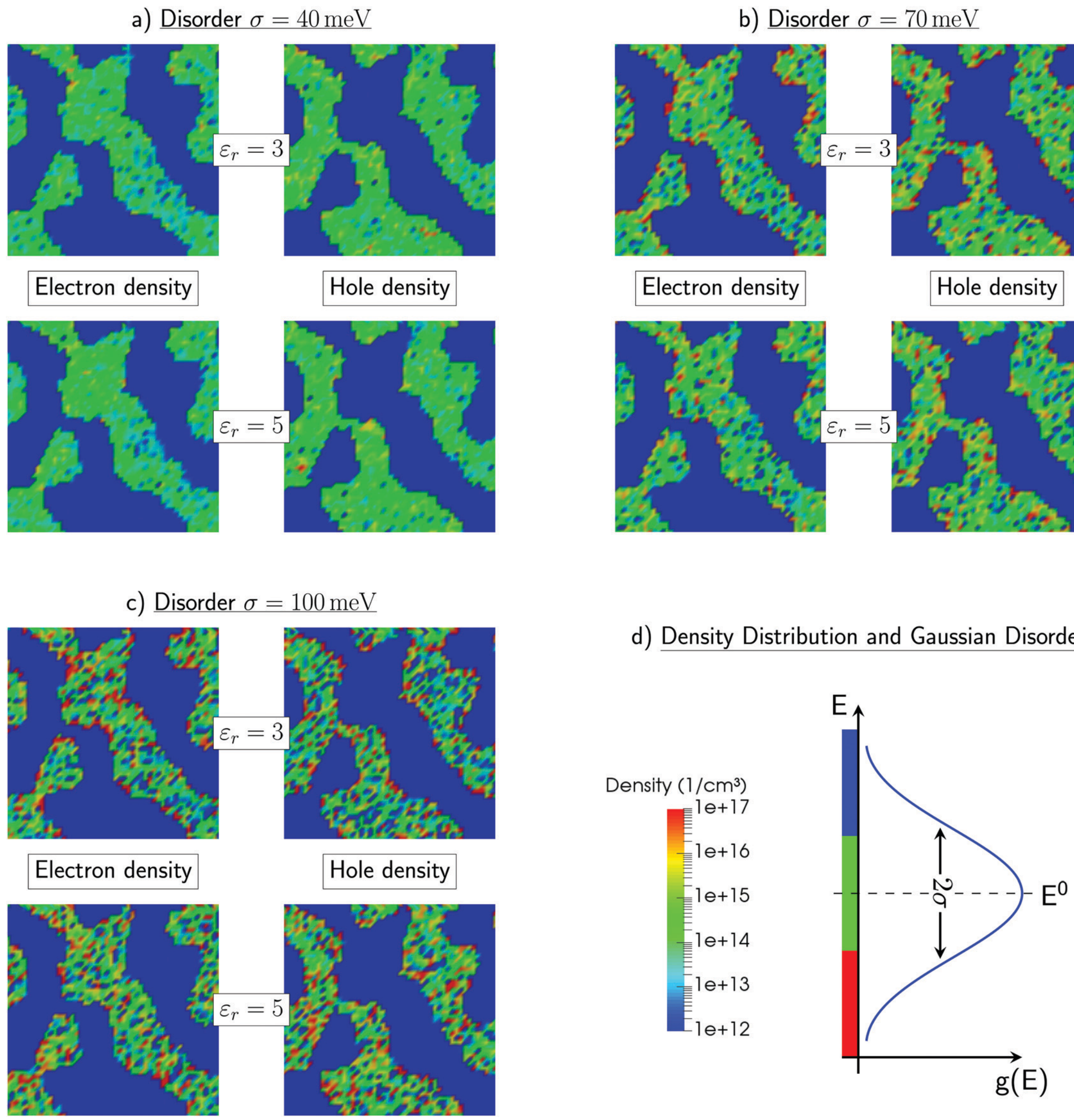

Fig. 1 Electron and hole charge density distributions along a slice through the morphology. All density maps are shown for two cases of low and high permittivity (ε_r = 3 and ε_r = 5), respectively, and the energetic disorder varies from 40 meV (a) *via* 70 meV (b) to 100 meV (c). In (d), the corresponding charge density scale and its relationship to the energy levels within the Gaussian density of states is shown.

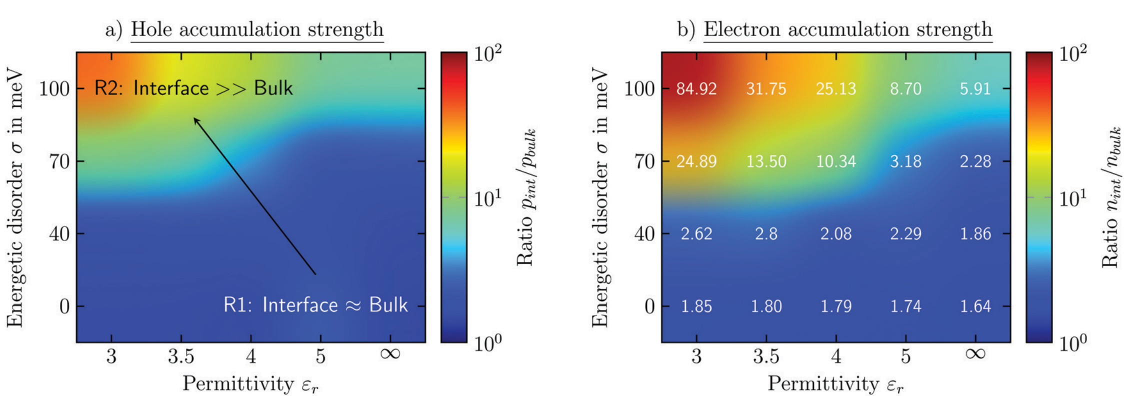

Fig. 2 Ratio of interface to bulk charge densities of holes (a) and electrons (b) for different parameter sets of energetic disorder and permittivity (σ, ε_r). High values indicate an inhomogeneous charge distribution with accumulation of charges at the heterojunction interface while a value of 1 represents homogeneous charge distributions of electrons in the acceptor and holes in the donor, respectively. The artificial case of $\varepsilon_r = \infty$ (no Coulomb interaction) is added to be able to interpret the effect of disorder alone.

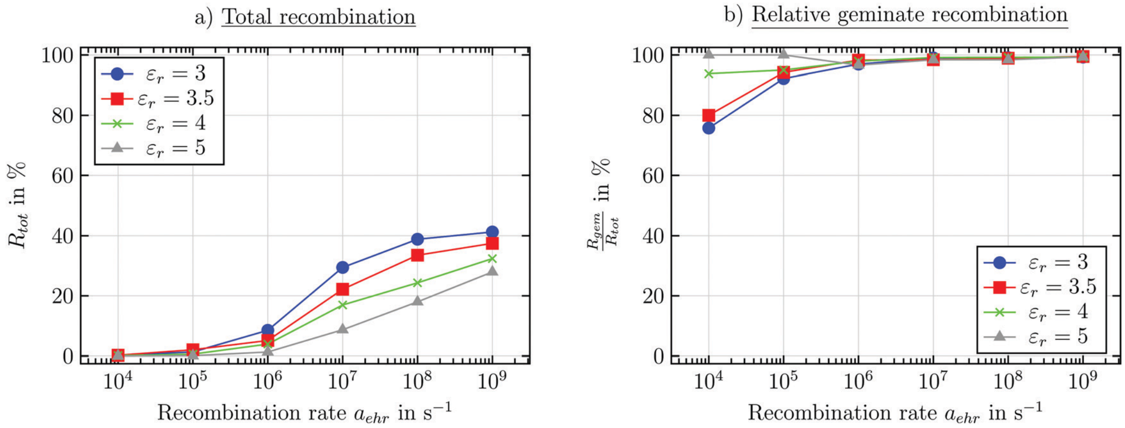

Fig. 3 Amount of total recombination R_{tot} (a) and the corresponding relative part of geminate recombination R_{gem}/R_{tot} (b) at σ = 70 meV depending on a_{ehr} at different values of ε_r. A value of R_{tot} = 100% means that all charges generated by exciton splitting undergo recombination. A value of R_{gem}/R_{tot} = 100% means that from all recombination events, every single one is geminate and none are nongeminate. All recombination that is not geminate is nongeminate recombination.

Table 1 Effect of permittivity and disorder on short-circuit current density j_{sc} in mA cm^{-2} for $a_{ehr} = 5 \times 10^4$ s^{-1}

	ε_r				
σ (meV)	3	3.5	4	5	∞
100	4.62	5.92	6.77	7.62	8.21
70	7.24	7.59	7.33	7.65	8.11
40	7.31	7.44	7.52	7.71	8.24
0	7.53	7.58	7.65	7.75	8.36

Table 2 Effect of permittivity and disorder on short-circuit current density j_{sc} in mA cm^{-2} for $a_{ehr} = 10^7$ s^{-1}

	ε_r				
σ (meV)	3	3.5	4	5	∞
100	0.95	2.08	3.24	5.18	8.08
70	5.08	5.72	6.15	6.85	8.10
40	7.45	7.51	7.54	7.69	8.13
0	7.47	7.51	7.66	7.86	8.35

At last, in order to link σ and ε_r on the device performance, Table 1 shows the effect of σ and ε_r at $a_{ehr} = 5 \times 10^4$ s^{-1} on the short-circuit current j_{sc} with the corrected values for σ = 0 meV, 40 meV, 70 meV, 100 meV; it replaces Table 1 of the original manuscript. We have furthermore added the dependence of j_{sc} on σ and ε_r for a larger recombination rate of $a_{ehr} = 10^7$ s^{-1} in Table 2, in order to show the effect at smaller recombination times. The trend is equivalent (*i.e.* the anti-correlation of interface accumulation strength and j_{sc}) but more pronounced, as a larger a_{ehr} induces faster and therefore more recombination.

There are no qualitative changes in the conclusions of the paper. However, considering the corrected results, we can conclude more suitable recombination rates around $a_{ehr} \approx 10^7$ s^{-1} at an energetic disorder of 70 meV and a permittivity of ε_r = 3.5.

Acknowledgements

The authors thank Waldemar Kaiser for spotting the mistake.

The Royal Society of Chemistry apologises for these errors and any consequent inconvenience to authors and readers.

References

1 I. A. Howard and F. Laquai, *Macromol. Chem. Phys.*, 2010, **211**, 2063.